Reinforced polyvinylidene fluoride and polyurethane electrospun layered nanofiber-based membranes for effective model water dead-end microfiltration

Dusan Kimmer*, Miroslava Kovarova, Muhammad Yasir, Lenka Lovecka, Jaroslav Cisar, Lenka Musilova, Josef Osicka and Vladimir Sedlarik

Centre of Polymer Systems, University Institute, Tomas Bata University in Zlín, Třída Tomáše Bati 5678, 76001 Zlín, Czech Republic

***Corresponding author:** D. Kimmer (kimmer@utb.cz)

Abstract

The research presented herein describes the preparation of electrospun homogeneous nanofibrous structures with customized morphology and properties, as well as textile supports for necessary reinforcement for microfiltration applications. Findings report membranes comprising polyurethane or polyvinylidene fluoride nanofibrous layer and polyethylene terephthalate nonwoven textile as support were evaluated. The investigation encompassed various constructions of materials, which include the influence of nanostructure morphology, the process of membrane cleaning by backwashing, and factors affecting flux, filtration efficacy, and working life. Application of membrane support made from polyethylene terephthalate with a large distribution of polymer chain provides a sufficiently strong connection with a layer of nanofibers with minimum penetration into the nanostructure involved in flux improvement. It was discerned that nanostructures with a morphology of 6 layers from thick (fiber diameter ~500 nm) and thin (fiber diameter ~180 nm) nanofibers with mean pore size 0.67 µm in comparison with membranes prepared from thin nanofibers only (mean pore size 0.26 µm exhibited improved flux (17 times higher after 150 min of filtration process). In contrast, the filtration efficacy of both membranes for filtering submicron particles remained stable and highly efficient. It also proved to smooth out the surfaces of the novel membranes, which simplified the removal of caked-up debris. Cleaning the filter by backwashing renewed the efficacy of the developed membranes for filtration and extended their working life. Finally, repeatedly backwashing the thin nanofiber layer membrane raised the water flux measured as 230 L m^{-2} h^{-1}, i.e., six times higher than without backwashing.

Keywords: Nanofiber; membrane; reinforcement; morphology; flux; backwashing

Introduction

Water is gaining importance as a strategic raw material, and its economic use is crucial [1]. About 40% of the global population inhabits areas with a lack of water, while 20% live where drinking water is contaminated. Estimates suggest this number will exceed 50% by 2025 [2]. The rationale and motive for this study were to develop novel, reinforced, nanostructured microfiltration (MF) membranes with improved properties that could contribute to overcoming issues connected with insufficient drinking water. Emphasis was placed on enhancing the flux of the microfiltration materials, extending their working life, and maintaining a desired level of filtration efficacy (FE). Numerous papers have been published over the past three decades on fabricating submicron fibers and their potential water treatment applications [3–6]. Polymeric nanofibers prepared by electrospinning result in an effective membrane material with the advantages of a large surface area, a high surface-to-volume ratio, and an interconnected porous structure [7–11].

A widely employed effective method for liquid purification is a pressure-driven separation process called microfiltration [12]. The pore sizes of microfiltration membranes vary between 0.1 and 10 µm in diameter, and such pores are uniformly distributed throughout the material. Conventional porous polymeric membranes possess intrinsic limitations, such as low flux, extensive fouling, and the undesirable formation of macro voids throughout their density. It appears, however, that electrospun nanofibrous membranes can overcome some of these drawbacks, as the pore sizes of microfiltration membranes can be controlled by varying specific parameters, i.e., the diameters of their nanofibers, pore sizes, and the temperature and pressure applied during the preparation stage. A membrane of this type is applicable as either a depth (dead-end filtration) or surface (cross-flow filtration) filter.

In *dead-end filtration,* the main direction of flow is perpendicular to the membrane. Suspended particles are continuously dragged towards it and deposited on the surface or inside its pores. Particles deposited in this manner build up, continuously increasing the resistance to flow and diminishing the permeate flux rate. A common way of mitigating these impacts is a process carried out in *cross-flow mode* (tangential flow), where the primary direction of flow is tangential to the membrane. This kind of flow essentially scours particles from the surface of the membrane, thus limiting particle deposition. Applying an MF membrane with a smooth, nanostructured surface would enhance the efficacy of the crossflow process.

Two main approaches exist for preparing nanofibrous MF membranes with controlled pore sizes, electrospinning conditions, and chemical or physical modification of the given material [13–15]. Thus, nanostructures exhibiting valuable properties for microfiltration are prepared, including high porosity, the random orientation of fibers, and weak interaction between fibers, which ushers in drawbacks of poor strength and toughness; unfortunately, this limits options for the practical application of MF membranes [16]. The diameters of fibers, their orientation, crystallinity, and bonding degree directly affect the mechanical properties of nanofibrous membranes [17]. In addition to boosting mechanical properties by the standard heat press method [18], alternative approaches to such improvement exist [19], e.g., adding fillers [20–23], thermal stretching [24–26], utilizing mixed solvents [27] or mixed polymers [28, 29], solvent vapor welding [15, 30], solvent-induced fusion of submicron fibers [27, 31–35], furthering fiber orientation [33, 34] and self-supported hydrogel filtration membranes [36].

The mechanical strength of nanofiber mats can be raised by depositing or laminating them onto conventional textiles or synthetic polymer substrates [35]. Polyethylene terephthalate (PET) is frequently utilized as membrane support to overcome the mechanical limitations of nanostructured membranes for water treatment. It functions well as a layer for capturing nanofibers [37, 38]. A material commonly employed in nanofiber collecting pads is polypropylene (PP) nonwoven textile (NT), which has also proven suitable as a membrane support [39].

MF membranes typically consist of two or three layers. A tough, nonwoven fibrous material forms the bottom one, providing mechanical strength and support to the upper layer, which has the required barrier or properties, while a third adhesive layer is often included between them: heat-activated adhesive coating on a given textile (for example by dot coating) or application of welding nets. After being repeatedly cleaned, the potential exists for the resultant composite textiles to retain their desirable characteristics, such as mechanical strength, nanofiber morphology, and fluid flux [40, 41]. However, it should be mentioned that the microfiltration area consisting of nanofibers is decreased because the thermo-activated adhesive fouls the nanostructure [18]. This explains why new approaches are needed to minimize the contact area between the nanofibers and the substrate. The application of a bicomponent NT or NT surface treated by polymeric melting glues causes a flow of melted glue into the nanostructure and, consequently, a reduction in the filtration area. The described novel method of anchoring polymeric nanostructure into support NT connects nanostructure

to support material with minimum loss of filtration area and effects on required membrane reinforcement.

This work describes the preparation of electrospun homogeneous nanofibrous structures with customized morphology and properties, as well as textile supports for necessary reinforcement. There are investigated practical approaches to enhancing the mechanical properties of nanostructured membranes by supplementing them with polyethylene terephthalate nonwoven textile containing polymeric chains which melt and soften at low temperatures, such as a type with a broad distribution of molecular weights (BD PET NT). Employing an electrospun nanofibrous membrane as a micro filter for purifying liquid requires the textile substrate to be reinforced to obtain a suitable strength, permeability, and smooth surface [42].

Fouling constitutes a significant issue when using MF membranes to treat contaminated water. This is a common phenomenon for MF membranes, hindering their efficacy for filtration, diminishing flux, and causing a high drop in pressure [43]. Nanofiber-based membranes outperform conventional membrane types in this respect due to their structure, choice of polymeric materials, and the possibility of using fouling-suppressing additives [36, 38, 44–49]. Extensive studies have been carried out, targeting photocatalyst immobilization in the nanofibrous structure to promote photocatalytic degradation of fouling and retention of open morphological structure towards exhibiting high performance in wastewater treatment [50]. Wastewater tertiary treatment based on Daphnia filtration as a polishing system was successfully developed for both particle removal and disinfection [51].

Nanofibrous microfiltration membranes have a higher flux, consuming less energy during application. As a consequence of their relatively high porosity and fully interconnected open-pore structure, this aspect lends them excellent permeability for water filtration. Microfiltration membranes are efficient in separating microparticles and bacteria from wastewater [52]. For instance, applying electrospun nanofibers with 100 nm diameters as a screen filter permits efficient separation of particles exceeding 300 nm in size [53]. A linear relationship exists between pore size and fiber diameter for membranes with a nonwoven structure and high porosity [54].

A practical method used to regenerate membranes, i.e., removing deposited particles or microorganisms from their surface, is washing, wiping, or shaking off. A membrane lacking a proper connection between its two layers, e.g., a thermal adhesive, can only be cleaned by the vibrating method, as backwashing for regeneration is unsuitable. The reason is pressure-

related delamination phenomena, which leads to the separation of the nanofiber layer from the membrane support.

Initial efforts were directed at reinforcing the material, after which samples were prepared that differed in the morphology of the nanostructure, while constructions varied in the placement of layers. Discussion is given on filtration efficacy, the influence of smoothing the upstream layer, flux, and changes in the latter induced by backwashing.

Materials and methods

All the chemicals utilized were of reagent grade. N, N-dimethylformamide (DMF), and toluene, employed as a solvent and cosolvent for the polymer solutions, were purchased from Lach-Ner (Czech Republic). Additives used to increase the conductivity of the polymer solutions, i.e., citric acid and sodium tetraborate decahydrate, were obtained from PENTA s.r.o. (Czech Republic); tetraethyl ammonium bromide came from Sigma-Aldrich (Germany).

The polymers comprised polyvinylidene fluoride copolymer with hexafluoropropylene (PVDF) Kynar-Flex 2801-00 by the Arkema Group and a solution of polyurethane (PU) Permuthane SU-22-542 purchased from Stahl Europe (The Netherlands).

Preparation of the nanofibrous structures

For the electrospinning of base nanofibrous layers for two- and five-layer membranes, the solutions of PVDF in DMF at the concentration of approx. 20% by weight was used. Electrical conductivity was increased to 150 $\mu S\ cm^{-1}$ by adding sodium tetraborate decahydrate and citric acid at the ratio of 1:3. The viscosity of the solution equaled 1.5 Pa s; the PVDF solution was utilized to prepare layers of nanofibers with the mean fiber diameter of approximately 170 nm. PVDF nanostructures at a width of 40 cm were fabricated from the polymeric solutions on a Spin Line 40 (SPUR, Czech Republic) electrospinning device equipped with 32 nozzles arranged in two lines for forming nanofibers.

A nanostructure (nNT = nano non-woven textile) comprising six layers of PU nanofibers, in an arrangement alternating between thin and thick fibers, was prepared from two PU solutions in DMF. The electrical conductivity of 20% solution for the thin nanofibers (mean fiber diameter of approx. 180 nm) was adjusted to 320 $\mu S\ cm^{-1}$, using the tetraethyl ammonium bromide for this purpose; the viscosity of the solution was 0.7 Pa s. The electric conductivity of the 20% PU solution in DMF and toluene for the thick fibers (mean fiber diameter of approx. 500 nm) equaled 37 $\mu S\ cm^{-1}$ without any additional conductivity adjustment; the

viscosity of the solution was 1.7 Pa s. The aforementioned PU nanostructures made up of alternating layers of thick and thin nanofibers were fabricated at the width of 120 cm on a Spin Line 120 (SPUR, Czech Republic) pilot line unit, operating with 96 nozzles arranged in 6 lines (spinning electrodes). The first, third, and fifth lines were fed with a higher electrical conductivity PU solution to make the thin fibers, whereas the PU solution for forming the thick fibers ran through the second, fourth, and sixth lines.

The PVDF or PU nanofibers were collected on PET NT, prepared from polymer with a large distribution of polymer chains (BD PET NT – Neaustima, Lithuania; 60 g m^{-2} in basic weight). The fundamental parameters of the electrospinning process and the resultant nanofibrous structures are presented in Table 1.

Table 1 Fundamental parameters of the electrospinning process and nanofibrous structures

Parameter	Unit	PVDF	PU thin/thick nanofibers
Voltage	kV	65–75	60
Current	mA	0.65	0.2
Dosing of polymer solution	mL min^{-1}	0.4	1.1 (1^{st}, 3^{rd}, 5^{th} line of nozzles)/ 0.9 (2^{nd}, 4^{th}, 6^{th} line of nozzles)
Substrate movement rate	m min^{-1}	0.1	0.2
Distance between electrodes	mm	200	210
Temperature	°C	23	24
Relative humidity	%	32	33
Basic weight of nanofibers	g m^{-2}	2.4	1.9
Mean fiber diameter	nm	170	180/500

Membrane preparation

In all cases, the nanofibers were deposited directly on the BD PET NT support substrate; the conditions for sample preparation are summarized in Table 2. The reinforced, two-layer membrane referred to as MFL consisted of PVDF nanofibers layered on the BD PET NT support textile (Figure 1A). It was pressed at 120–135 °C at a pressure of 600 kPa for a contact time of 10 seconds. A glossy separative paper (Multicast, Arjowiggins, Spain) was employed to obtain a smooth surface on the nanostructured membrane.

In order to achieve even better stiffening and ensure a still smoother surface on both sides of the membrane, a five-layer membrane was made, referred to as $(MFL)_2$3L (Figure 1B). This involved laminating together two MFL membranes and a polyalkene trilaminate (PE-PP-PE) stiffening mesh (Claf, JX Nippon, Japan), the latter being sandwiched between the rear surfaces of two MFL membranes; lamination occurred under a pressure of 600 kPa at 135 °C for 20 s.

Another membrane fabricated in a similar manner was based on PU nanofibers (MPU), wherein layers of thick and thin nanofibers were arranged in a six-layer nanostructure (Figure 1C); a laminating line at the width of 120 cm by Maschinenfabrik Herbert Meyer GmbH, (Tomatex, Czech Republic), was employed for this purpose.

Table 2 Compositions of the membranes tested

Sample designation	Unit	MFL	$(MFL)_2$ 3L	MPU
Support		BD PET NT	BD PET NT	BD PET NT
Chemical composition of nanofibers		PVDF	PVDF	PU
Basic weight of nNT	g m^{-2}	2.4	2 × 2.4	1.9
Nanofiber diameter	nm	170	170	180/500
Number of layers		2	5	2
Layering		nNT on PET	nNT on PET/ PE-PP-PE trilaminate/ PET with nNT	alternating 3 thick and 3 thin nNT on PET
Temperature of pressing	°C	120-135	135	125*
Lamination pressure	kPa	600	600	400*
Contact time	s	10	20	15*

* Meyer lamination line at a speed of 4 m min^{-1} with a slot of 0.5 mm.

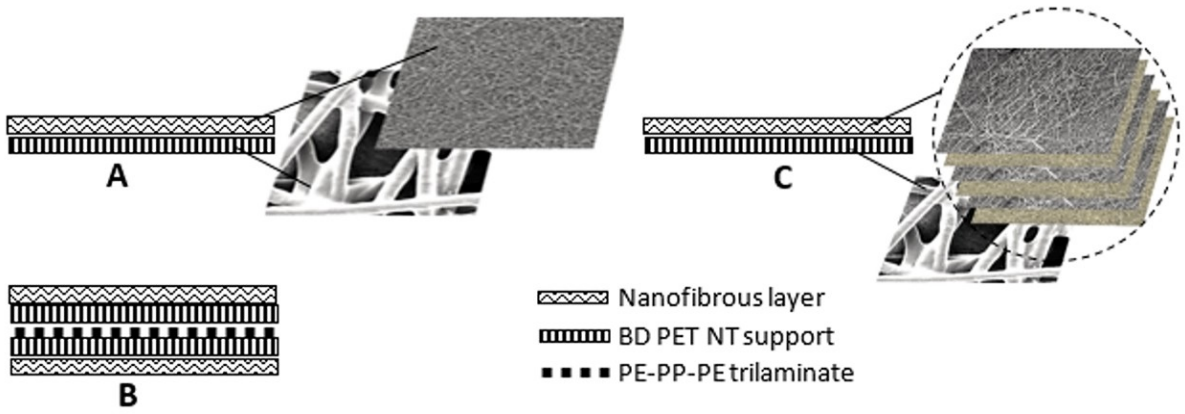

Figure 1 Applied membrane constructions consisting of BD PET NT support and PVDF nanofibers arranged in two (A) or five layers (B) and BD PET NT support with PU nanostructure formed from six layers of thick and thin PU nanofibers (C).

Characterization of the Membranes

The membranes were characterized in terms of the morphology of their nanofibrous layers, basic weight, pore size characteristics, measurement of flux, and filtration properties. Thermal analysis of the substrate material was also performed.

The nanostructure morphology was analyzed in the membranes by scanning electron microscopy (SEM) on a Vega 3 unit (Tescan, Czech Republic). The samples were coated with a thin layer of palladium to increase their electric conductivity prior to taking SEM images.

Characteristics relating to the pore sizes of the membranes were assessed on a flow porosimeter (SPUR, Czech Republic) in accordance with ASTM F316-03 (2011); Galpor (Porometer NV, Belgium) was used as a wetting liquid. Dry and wet tests were conducted on three circular samples cut out from the given materials, and mean values were reported for them. The resulting porosimetry measurements encompassed the mean pore diameters of the nanostructures, the maximum pore diameter, and the permeability of the nanostructured membranes for dry air. Pore size distribution was counted as well.

The thermal behavior of the PET support materials was evaluated by differential scanning calorimetry (DSC) on a DSC 1 STAR (Mettler Toledo, Belgium) instrument. All measurements during thermal analysis were studied in an inert nitrogen atmosphere (50 mL min^{-1}). The rate of heating and cooling was set at 10 °C min^{-1}. The samples were initially heated from +25 °C to 270 °C, kept at 270 °C for 5 minutes to erase their thermal history, and then cooled to -30 °C; the second heating cycle ranged from -30 °C to 300 °C.

Mechanical testing of layered and reinforced membranes was carried out on samples with dimensions of 50×300 mm. The measurement was done on the tensile-testing machine Testometric MT350-5CT (Testometric, Rochdale, UK) according to EN ISO 2903-3 standard with an active length of 200 mm. Prepared samples were tested at a speed of 100 $mm.min^{-1}$ with a pre-load of 0.2 N. Six measurements were done for each type of membrane sample.

The model filtrated medium utilized in all the experiments was utility water (UW), which contained high iron salts and oxides (dry extract of solids equaled 0.23% by weight). A magnetic stirrer or pump was employed to scatter and disperse solid particles in the water homogeneously.

The apparatus for gauging flux at the hydrostatic pressure of 20 kPa consisted of a 2 m long water column tube and a module, the latter comprising two rectangular membranes (600×200 mm) adhered to a PP frame by silicone sealant and separated from each other by a wire pad to prevent contact during backwashing (Figure 2). An opening with a diameter of 5 mm functioned as an outlet for permeating from the space between the membranes. These plastic frame modules with fixed membranes were wetted for 3 hours in drinking water. Cycles

occurred for 4-5 minutes of flux at 20 kPa pressure, while the aforementioned backwashing test required the additional step of about 1 minute of backwashing at 20 kPa.

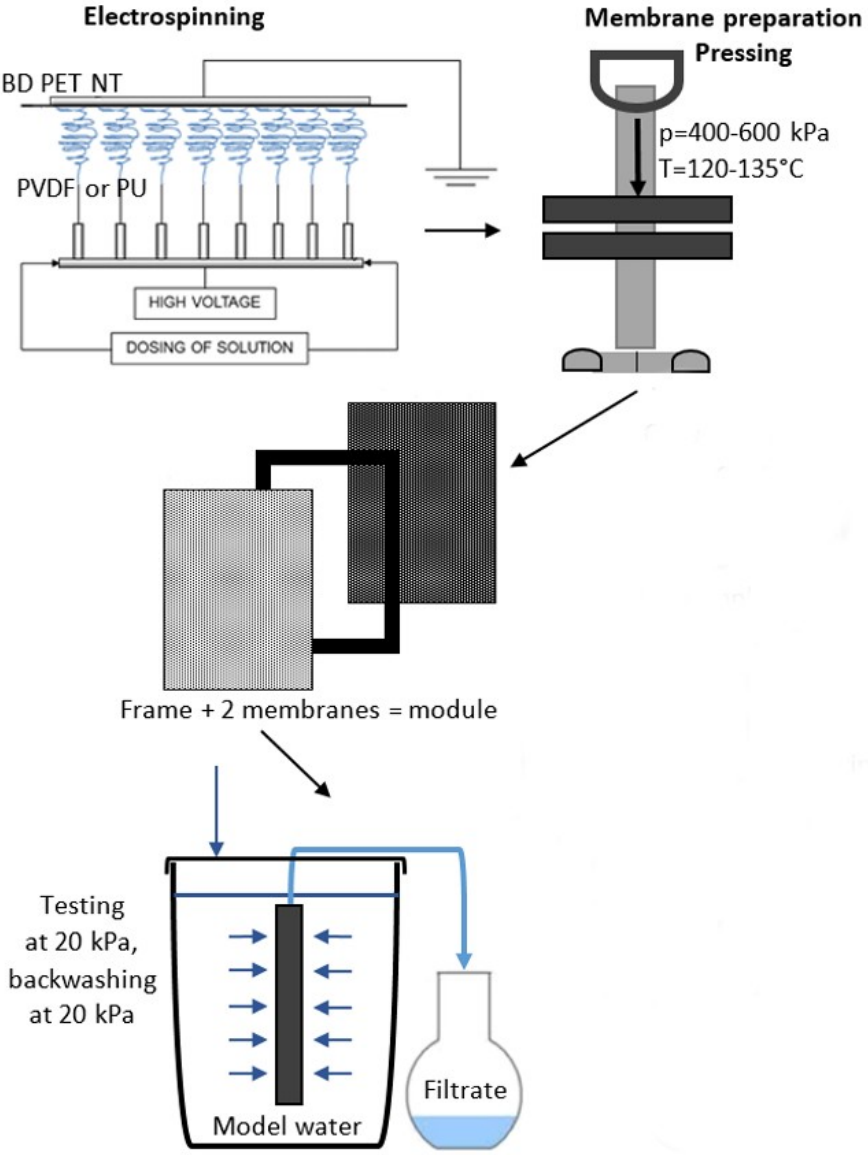

Figure 2 Membrane preparation and arrangements of filtration tests.

The filtration efficacy of the membranes was evaluated by determining the mean sizes of particles before and after filtering experiments. Laser diffraction (LD) and dynamic light scattering (DLS) were carried out for this purpose; the latter detects particles ranging from 0.3 nm to 10 µm, whereas LD gauges particles of 0.01 µm to 3500 µm in size. DLS was performed on a Zetasizer Nano ZS unit (Malvern, UK), which detected the intensity of diffused light at the angle of 173° and temperature of 25 °C. A Mastersizer 3000 device (Malvern, UK) was employed for the LD analysis, wherein red (633 nm) and blue (470 nm) laser rays were applied at laboratory temperature. The blue ray lent greater accuracy to the

measurement of submicron particles since the wavelength of its light in the diffraction of electromagnetic radiation was comparable to the sizes of such particles. The values presented are mean particle sizes calculated from five separate measurements taken for each sample.

Results

Membrane reinforcement

Excellent results were obtained by applying the support material (substrate), which was based on a PET NT created from polymer chains with a broad distribution of molecular weights. Such a distribution ensured the low molecular weight fraction of the PET softened and melted during the heat-pressing process, giving rise to a good connection between the nanofibers and reinforcing support of the membrane (Figure 3A and B) [55]. Heat pressing of the BD PET NT substrate with a 2.4 g m^{-2} layer of PVDF nanofibers across the range of temperatures of 120–140 °C caused fixation between the nanofibers and partially melted PET polymer chains, affording a good connection between the nanostructured and support layers. The membranes that possessed a smooth surface afterward could be cleaned by backwashing. Upon reaching the temperature of 160 °C, however, the nanostructure of the membranes had become deformed, i.e., partially melted (Figure 3C). The effects on pore size and air permeability exerted by the applied temperatures when preparing the membranes are detailed in Figure 4.

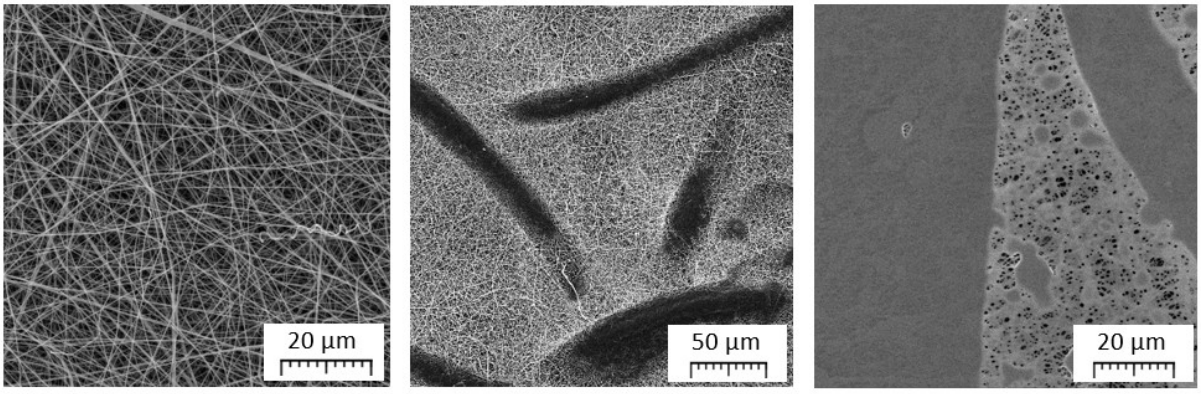

Figure 3 Influence of temperature on PVDF nanostructures affixed to the BD PET NT microfibers: A) a layer of default nanofibers; B) a surface of MFL membrane formed at 130 °C, with nanofibers adhered to the BD PET NT substrate; C) the broken surface of a nanostructure formed at 160 °C.

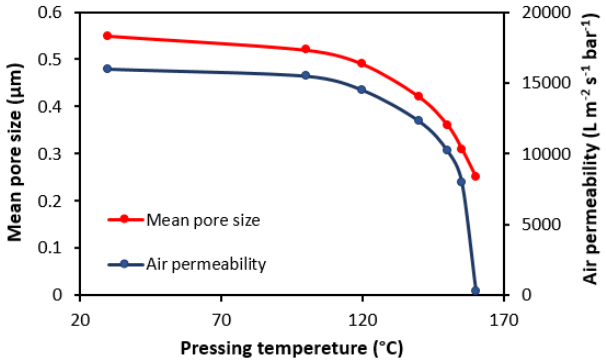

Figure 4 Decrease in membrane pore size and air permeability during the heat-pressing process.

Figure 5 contrasts differential scanning calorimetry charts for the partially degraded, recycled PET with a broad distribution (BD) of molecular weights and PET with a narrow distribution (ND) of molecular weights (ND PET). The comparison took place with the aim of comprehending the process behind the reinforcement of the membrane. Partial melting of low molecular fractions in the BD PET NT occurred at 146 °C, with the likelihood of softening at still lower temperatures, while the ND PET started at 209 °C. This variance in temperature is pertinent when preparing reinforced MF membranes where nanofibers are affixed to the surfaces of the PET microfibers. Minimal loss in the active filtration area transpires in relation to this connection, much less than when a thermo-activated adhesive is utilized, as the melted adhesive flows into the nanostructure. The DSC data in Figure 5 illustrates the differences in the initial melting temperatures of crystalline phase two of the PET polymers. Membranes prepared from PET with a higher melting temperature (generally exceeding the softening temperature of the polymer utilized in the preparation of the nanofibers) were unable to connect with the nanofibers properly; the filtration layer could be easily removed from the membrane by the stream of backwashing water.

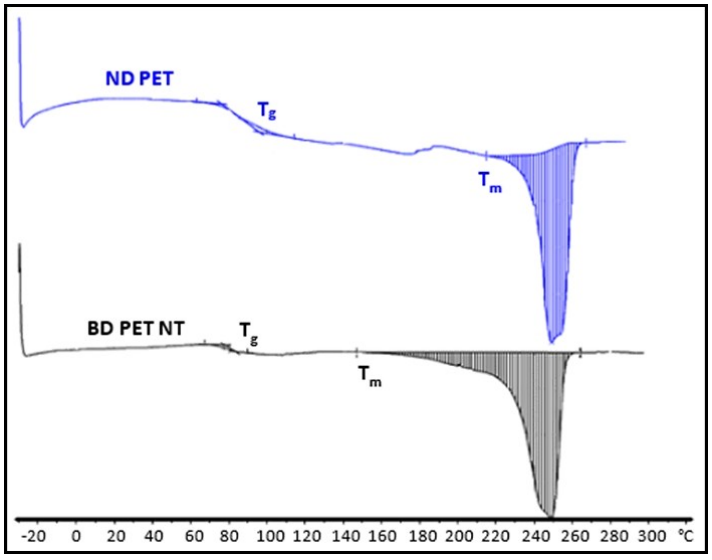

Figure 5 DSC data from the second heating cycle, as measured on the BD PET NT and ND PET.

The enhancement in the mechanical properties of the BD PET NT reinforced membrane (10 s pressing at 130°C and a pressure of 0.6 MPa) in comparison with thermal and pressure untreated layered membrane is demonstrated in Table 3 and Figure 6. The MFL membrane pressed of two layers (reinforcement and nanostructure) exhibits about a 16-fold increase in Young´s modulus, 7-fold enhancement in stress at break, and 2 times improvement in ultimate strength. The values of strain at break are comparable, as expected.

Table 3 Average values of mechanical properties of layered and reinforced membranes

Mechanical property	Young´s modulus	Stress at break	Strain at break	Ultimate strength
Unit	MPa	MPa	%	N
Reinforced membrane	311.2±39.5	12.9±1.0	25.0±2.2	93.1±8.4
Layered membrane	20.1±3.3	1.9±0.3	29.8±2.2	48.4±3.7

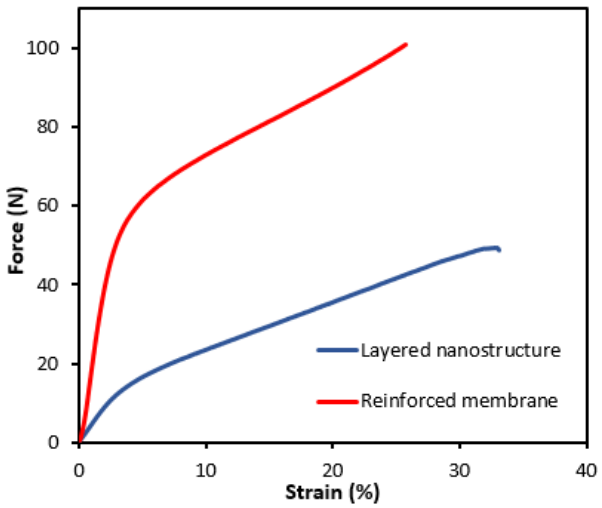

Figure 6 The course of force during the mechanical tensile test as a function of strain at a speed of 100 mm min^{-1} for layered (blue) and reinforced (red) membrane.

Porosity of the reinforced microfiltration membranes

The small diameters of the nanofibers lent them a degree of flexibility, in addition to which their nanostructures, being open and porous in morphology, ensured high flux for fluids. A strong correlation existed between filtration performance and the physical parameters of the nanofibrous membrane, such as membrane thickness, fiber diameter, and distribution of the same, which determined the pore size and related distribution across the membrane. The following characterizations of the membrane solely pertain to materials based on BD PET NT since they demonstrated the best reinforcing effect with potential for industrial application. Table 4 and Figure 7 present characteristics of pore size determined for the MF membranes,

which underwent dry and wet tests following ASTM F316–03. The most critical aspects of the porosity of the nanostructure are its essential weight and fiber diameter, which significantly affect the mean diameter of the inherent pores, the maximum diameter of the pores, the permeability of the nanostructure for dry air, and the pore size distribution. Each material under inspection was designated according to the value for mean fiber diameter. In this context, values are reported for the following: two-layer membranes referred to as MFL 0.41 and MFL 0.26, which differed in mean pore size (0.41 µm and 0.26 µm, respectively); five-layer membrane labeled as $(MFL)_2$3L with a mean pore size of 0.21 µm; and membrane MPU 0.67 made up of 6 alternating layers of thick and thin PU nanofibers, with a mean pore size 0.67 µm.

Table 4 Filtration characteristics of the MF membranes

Nanostructured membrane	Unit	MFL 0.26	MFL 0.41	$(MFL)_2$3L 0.21	MPU 0.67
The basic weight of the nanostructure	g m^{-2}	2.4	2.4	2×2.4	1.9
Mean pore diameter[A]	µm	0.26	0.41	0.21	0.67
Maximum pore diameter[B]	µm	0.34	0.52	0.26	1.00
Permeability for dry air	L min^{-1} bar^{-1} cm^{-2}	32	59	22	103

[A] standard deviation ±10%
[B] standard deviation ±8%

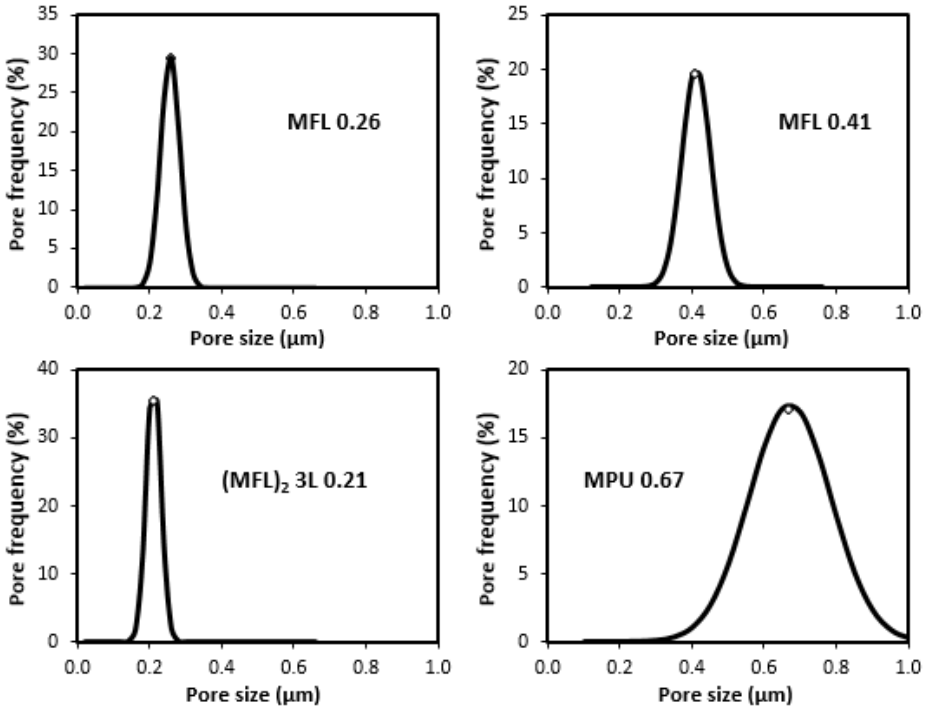

Figure 7 Pore size distributions of the MF membranes utilizing the BD PET NT support.

Preparing the MFL 0.26 membrane involved the additional heat pressing of MFL 0.41 at 135°C, which is why it possessed lower values for the mean diameter of pores and a narrower pore size distribution. Comparing the characteristics of the MFL 0.41 and MFL 0.26 membranes confirmed the expectation that pressing at a higher temperature would vary pore size. However, a decrease in the mean value of this through the application of heat pressing had limits. Indeed, the authors were unsuccessful at fabricating ultrafiltration membranes with a mean pore size of less than 100 nm by heat pressing a microfiltration nanostructure consisting of nanofibers.

A five-layer membrane was prepared from two MFL membranes fixed together with PE-PP-PE trilaminate mesh. The membrane possessed a smooth nanostructured layer on both sides, meaning that any retentate could be removed simply from an inlet site while its outlet site would clog up less when backwashing.

An MPU membrane was formed by alternating layers of thick and thin PU nanofibers (6 layers with essential weight each of ca 0.3 g m^{-2}) on the BD PET NT support and conducting subsequent lamination. The nanostructures were affixed properly in the PET support; however, the inlet side of the MPU membrane made up of thick fibers was more open. Since the mean and maximum pore diameters were high (0.67 and 1.00 µm, respectively), it was expected that flux would be, too.

Influence of membrane Construction and Nanostructure morphology on Utility Water Filtration

The test was performed on four different nanostructured MF membranes with a BD PET NT support fastened to purpose-built plastic frames to form a plate module (Figure 2). The modules were immersed in filtered utility water (UW) with the presence of contaminants (0.23% by weight, primarily oxides and salts of iron). Experiments were devised to discern the influence of membrane construction and nanostructure morphology on the flux of the MF membranes. Figure 8 contains a graph plotting the dependence of flux against the filtration time of the samples.

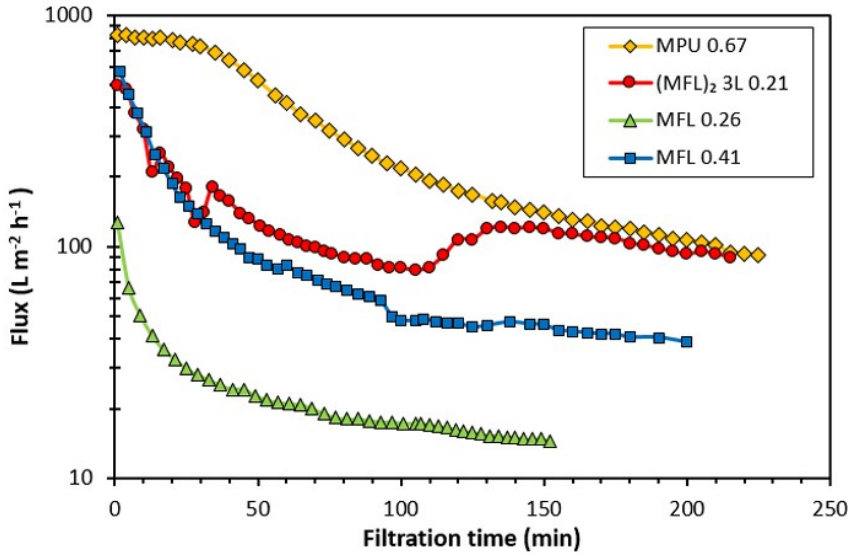

Figure 8 Flux through the MF membranes at the pressure of 20 kPa.

Table 5 details the total amounts of UW filtered through 0.24 m^2 of the area of the membrane and fluxes expressed in L m^{-2} h^{-1} after 150 and 215 minutes of the filtration process. The best results were achieved using the membrane based on thick and thin nanofibers (MPU) since alternating layers with larger and smaller pores helped to increase the flow.

Table 5 Filtration capacity of the MF membranes

Nanostructured membrane	Unit	MFL 0.26	MFL 0.41	$(MFL)_2$3L 0.21	MPU 0.67
Quantity of UW that flowed after 150 min	L	14.1	68.5	83.6	242.1
Flux after 150 min	L m^{-2} h^{-1}	14.8	46.0	119.5	140.3
Quantity of UW that flowed after 215 min	L			110.3	276.1
Flux after 215 min	L m^{-2} h^{-1}			91.5	101.5

The dependencies plotted in Figure 8 confirmed that flux through the two-layer MFL membrane with a larger mean pore size was significantly higher than through a membrane with finer pores. The quantity of UW that flowed through membrane MFL 0.41 after 150 minutes at 20 kPa was 4.9 times greater than for MFL 0.26. The finding that higher fluxes were achieved with the five-layer membrane $(MF)_2$3L could be surprising, considering its lesser mean pore size of just 0.21 µm; air cavities around the polyalkene trilaminate in the middle of it played a positive role in this.

The best flux was observed for the MPU membrane, as its mean pore size of 0.67 µm would suggest. The quantity of UW that had passed through the MPU 0.67 membrane after 150 minutes of dead-end filtration was 2.9 times higher than for the five-layered $(MFL)_2$3L

0.21 membrane, 3.5 times over MFL 0.41 and 17.2 times greater than MFL 0.26. The morphology of alternating layers of thick and thin nanofibers in a six-layer nanostructure resulted in higher values for flux at the commencement of filtration for the PU membrane than the rest. Although the MFL membranes have a smooth surface that reduces the build-up of a filter cake during the filtration experiment (fall away of filtration debris correlating with the wave-like curve for flux), the particles filtered by the MPU membrane with a six-layer nanostructure become stuck in the nanostructure as depicted in the SEM image in Figure 9B. This is because the nanostructure applied on the inlet side for UW filtration is formed by thick nanofibers (Figure 9A). The findings for flux through the $(MFL)_2$3L 0.21 and MPU 0.67 membranes after 215 minutes of dead-end filtration are almost identical, probably as a consequence of frequent removal of filter cake (sudden changes on flux curve for $(MFL)_2$3L membrane) from the smooth surface of $(MFL)_2$3L and the gradual clogging of the MPU membrane.

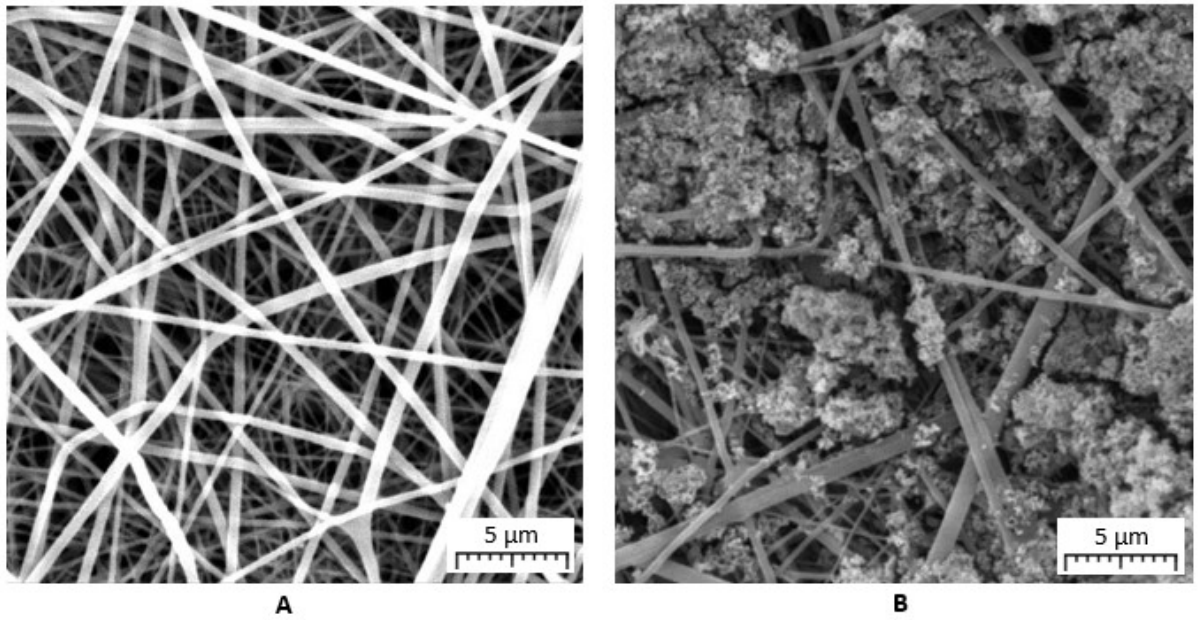

Figure 9 The six-layer PU nanostructure of thick (on the top) and thin nanofibers A) before the filtering process and B) after the filtration of UW.

Filtration efficacy

A comparison was made for the PVDF-based membrane $(MFL)_2$3L, which was anticipated to have the best filtration efficacy, and the PU-based membrane (MPU), with potentially worse capability, thereby revealing significant differences in the morphological arrangement of the nanostructures. Unfortunately, it was not possible to electrospin a membrane with a PVDF nanostructure of alternating layers of thick and thin nanofibers.

A matter of great interest was finding out if the layered arrangement of the nanofibrous structure of the PU membrane impacted the filtration process in any way; the techniques of LD and DLS were employed to this end. The graph in Figure 10A shows the dependence of volumetric particle size distribution on the size of particles in the UW prior to filtration through the $(MFL)_2$3L 0.21 and MPU 0.67 membranes. Figure 10B details the determination of volumetric distributions concerning particle sizes (in µm) for five samples, and the findings proved that the testing method applied was both very reliable and repeatable.

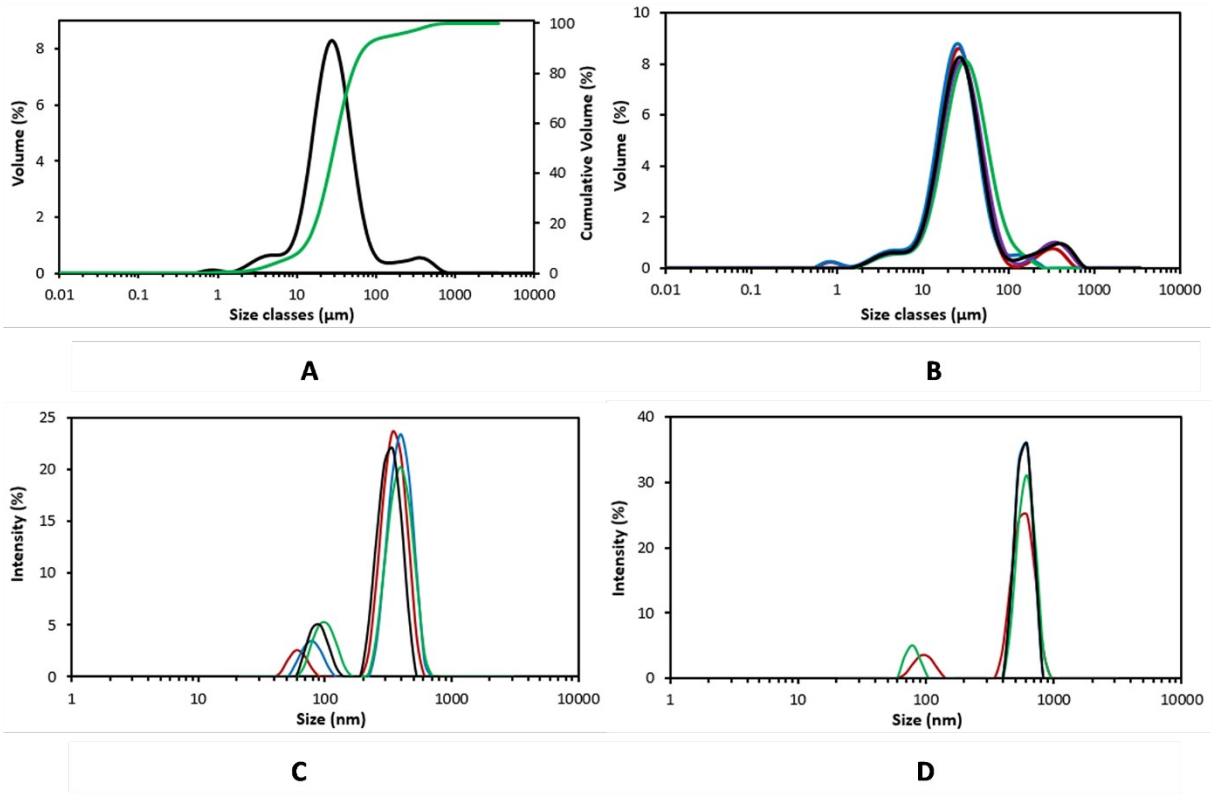

Figure 10 A) Volumetric particle size distribution concerning particle size in the UW used for filtration, as gauged by LD B) reproducibility of determination volumetric particle size distributions concerning particle sizes of UW used for filtration, as assessed by LD C) intensity-weighted particle size distribution after 215 min of filtration through $(MFL)_2$3L 0.21 membrane, as gauged by DLS D) intensity-weighted particle size distribution after 226 min of filtration through MPU 0.67 membrane, as gauged by DLS.

Analysis by DLS of the particle size distribution (in nm) in the permeate after filtration through the membranes as intensity-weighted distribution is given in Figures 10C and 10D. The lowest Z-average of particle size (661±46 nm) was observed for $(MFL)_2$ 3L (see Figure 10C). The permeate contained two populations of particles, one of size 370±34 nm accounting

for 84% of particles in the permeate, and another of particle size 82±20 nm for the remaining 16%. The corresponding values for the MPU membrane (Figure 10D) with six altering layers of nanofibers were 590±35nm (94%) and 87±6 nm (6%). The filtration efficacy of $(MFL)_2$ 3L concerning particle size exceeded that of the MPU membrane, as anticipated. Nevertheless, the sizes of particles filtered by the PU membrane (mean pore size 670 nm) were surprisingly low. The presence of finer fibers in three layers of MPU nanostructure can ensure good filtration efficacy. The morphological arrangement of the six-layer MPU nanostructure facilitated heightened filtration efficacy, so no significant changes in final values for consequent filtration efficacy were observed in comparison with MFL membranes.

Module filtration of utility water with repeated backwashing

The SEM images in Figure 11 A-C reveal the varying state of the MFL 0.41 membrane during the filtration test. The filtering medium was UW with the presence of solids (equal to the dry extract of 0.23% by weight).

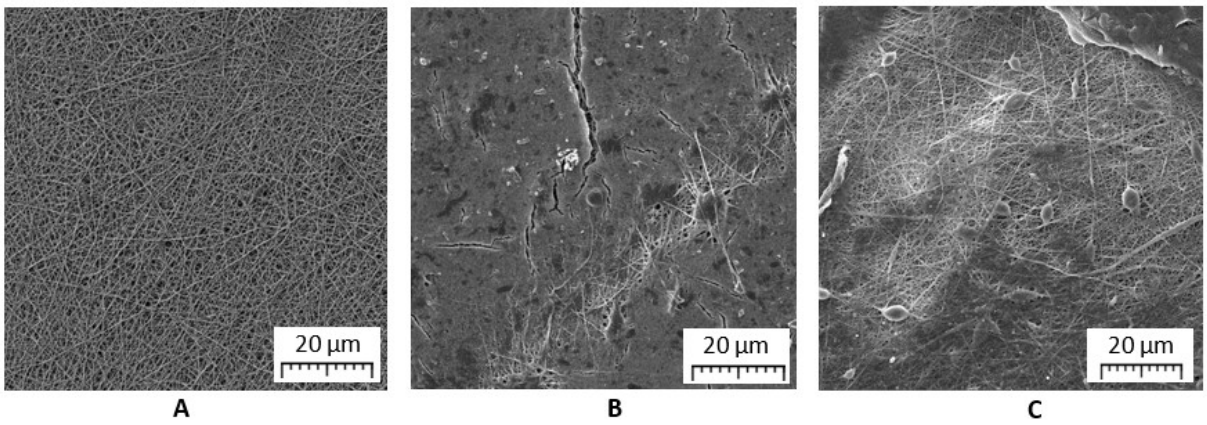

Figure 11 SEM images of the nanostructured MFL 0.41 membrane; A) the nanofibers of the prepared MFL membrane prior to filtration; B) clogging after two hours of filtration; C) the surface after backwashing.

An investigation was conducted involving repeated backwashing to raise the capacity for UW filtration by devising a module based on plastic frames equipped with the MFL 0.41 membrane. The filtering cycle comprised 4-5 minutes of flux and 1 minute of backwashing, both at the pressure of 20 kPa. Backwashing facilitated an approximate six-fold rise in flux between 220 L min^{-2} h^{-1} to 280 L min^{-2} h^{-1} after 3 hours of filtration, in comparison with the 40 L min^{-2} h^{-1} measured for the module without backwashing (see Figure 12). All the novel smoothed-out MF membranes showed no permanent tendency to foul, meaning their performance could be partially recovered by backwashing with clean water, depending on the size of the particles being filtered. The opposite backwashed sites of all the tested

microfiltration membranes after filtration were observed to be clean, i.e., white without any red dots of iron particles that indicate defects in the material.

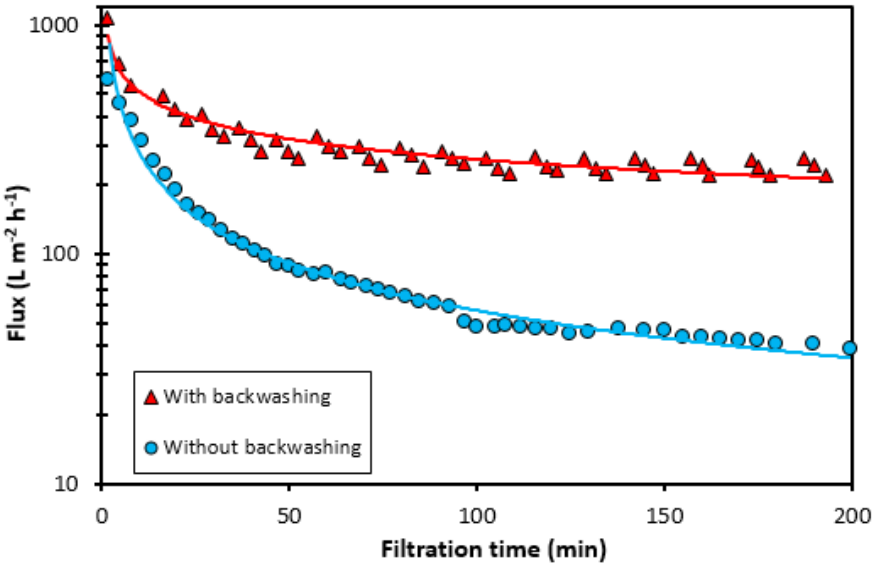

Figure 12 Clogging of the MFL 0.41 membrane by UW with and without backwashing at 20 kPa.

Discussion

The primary purpose of this study was the preparation of a microfiltration membrane with maximum flux and concurrently maximum filtration efficacy. The application of PET membrane support with the requested content of polymeric chains melting at lower temperatures provided membrane reinforcing with minimum loss of nanostructured filtration area. Processing variables to reach suitable membrane reinforcing were a temperature of 120°C, a pressure of 0.6 MPa, and a pressing time of 10 s. Pressing at a higher temperature or applying pressure for a longer time would vary pore size, which decreases the flux, but the surface of the membrane is becoming smoother and easily cleaned by backwashing or streaming of water.

It has been found that flux can be positively influenced by membrane construction (layering thick and thin nanofibers), whereas high filtration efficacy was maintained. The LD and DLS techniques have been found as a very useful tools for assessment of filtration efficacy (separation of submicron particles from water) by means of nanostructured membranes. The right combination of particular processing variables can be used to tailor nanostructured microfiltration membranes.

Conclusions

PVDF and PU membranes were successfully prepared using the electrospinning technique and characterized for model utility water microfiltration. Out of the various methods that exist for treating water, advanced membranes have the most significant potential to solve difficulties relating to matter across the globe. Applying nanostructures comprising a combination of thin and thick nanofibers enhanced the flux of the microfiltration membranes. It ensured high filtration efficacy for submicron particles, which was proven by gauging particle distribution prior to and following filtration. The quantity of utility water that flowed through a type of membrane consisting of thick and thin layers of nanofibers (MPU), was up to 17 times greater in the given test interval (150 min) in comparison with a membrane prepared with a basic unique nanostructure morphology (MFL). Limitations are experienced when applying nanostructured membranes consisting of nanofibers relating to tensile strength and toughness. Utilizing a support substrate enhanced the applicability of the nanostructured membranes, herein a PET nonwoven textile with a broad distribution of molecular weights. The novel approach developed of connecting a nanostructure and supporting layer resulted in minimal loss of the nanostructured area for filtration, which brought a smooth membrane inlet site, which facilitated the removal of filter cake. This was cleaned by backwashing, thereby restoring the flux of the material, decreasing the tendency for clogging and lengthening the working life of the microfiltration membranes. Repeated backwashing raised the flux of utility water through the two-layer nanostructured membrane at a settled state around 230 L m^{-2} h^{-1}, six-fold higher than without backwashing. The novel smoothed MF membranes exhibited no permanent tendency for fouling at high flux levels compared to commercial alternatives. Thus, modified membrane can potentially be used for efficient wastewater treatment applications.

Data and code availability

The raw data that supports the findings of this study are available from the corresponding author upon reasonable request.

Acknowledgements

The authors gratefully acknowledge the financial support from the Ministry of Education, Youth, and Sports of the Czech Republic (DKRVO RP/CPS/2024-28/002). We would also like to acknowledge the Centre of Polymer Systems (CPS) situated at Tomas Bata University in Zlin, Czech Republic, to use the available research facilities to conduct this research work.

Author contributions

Dusan Kimmer: conceptualization, methodology, investigation, writing – original draft, project administration; **Miroslava Kovarova:** validation, investigation, writing - review & editing; **Muhammad Yasir:** writing and reviewing, **Lenka Lovecka:** investigation; **Jaroslav Cisar:** formal analysis, data curation; **Lenka Musilova:** formal analysis, data curation; **Josef Osicka:** formal analysis, data curation; **Vladimir Sedlarik:** supervision, project administration, funding acquisition.

Declarations

Conflicts of interest The authors declare that they have no known competing financial interests or personal relationships that could have appeared to influence the work reported in this paper.

Ethical approval Not applicable.

Supplementary information Not applicable.

References

1. Tofighy MA, Mohammadi T, Sadeghi MH (2021) High-flux PVDF / PVP nanocomposite ultrafiltration membrane incorporated with graphene oxide nanoribbones with improved antifouling properties. J Appl Polym Sci 138:49718. https://doi.org/10.1002/app.49718

2. Wang X, Hsiao BS (2016) Electrospun nanofiber membranes. Curr Opin Chem Eng 12:62–81. https://doi.org/10.1016/j.coche.2016.03.001

3. Klaessig F, Marrapese M, Abe S (2011) Current Perspectives in Nanotechnology Terminology and Nomenclature. In: Murashov V, Howard J (eds) Nanotechnology Standards. Springer, New York, NY, pp 21–52

4. Teo WE, Ramakrishna S (2006) A review on electrospinning design and nanofibre assemblies. Nanotechnology 17:R89–R106. https://doi.org/10.1088/0957-4484/17/14/R01

5. Nguyen LTH, Chen S, Elumalai NK, et al (2013) Biological, Chemical, and Electronic Applications of Nanofibers. Macromol Mater Eng 298:822–867. https://doi.org/10.1002/mame.201200143

6. HMTShirazi R, Mohammadi T, Asadi AA, Tofighy MA (2022) Electrospun nanofiber affinity membranes for water treatment applications: A review. J Water Process Eng 47:102795. https://doi.org/10.1016/j.jwpe.2022.102795

7. Kimmer D, Vincent I, Fenyk J, et al (2011) Morphology of Nano and Micro Fiber Structures in Ultrafine Particles Filtration. Zlin, (Czech Republic), pp 295–311

8. Kimmer D, Vincent I, Lovecka L, et al (2017) Some aspects of applying nanostructured materials in air filtration, water filtration and electrical engineering. Zlín, Czech Republic, p 060001

9. Reneker DH, Chun I (1996) Nanometre diameter fibres of polymer, produced by electrospinning. Nanotechnology 7:216–223. https://doi.org/10.1088/0957-4484/7/3/009

10. Huang Z-M, Zhang Y-Z, Kotaki M, Ramakrishna S (2003) A review on polymer nanofibers by electrospinning and their applications in nanocomposites. Compos Sci Technol 63:2223–2253. https://doi.org/10.1016/S0266-3538(03)00178-7

11. Kimmer D, Slobodian P, Petráš D, et al (2009) Polyurethane/multiwalled carbon nanotube nanowebs prepared by an electrospinning process. J Appl Polym Sci 111:2711–2714. https://doi.org/10.1002/app.29238

12. Ulbricht M (2006) Advanced functional polymer membranes. Polymer 47:2217–2262. https://doi.org/10.1016/j.polymer.2006.01.084

13. Kaur S, Ma Z, Gopal R, et al (2007) Plasma-Induced Graft Copolymerization of Poly(methacrylic acid) on Electrospun Poly(vinylidene fluoride) Nanofiber Membrane. Langmuir 23:13085–13092. https://doi.org/10.1021/la701329r

14. Moslehi M, Mahdavi H (2020) Preparation and Characterization of Electrospun Polyurethane Nanofibrous Microfiltration Membrane. J Polym Environ 28:2691–2701. https://doi.org/10.1007/s10924-020-01801-z

15. Huang L, Arena JT, Manickam SS, et al (2014) Improved mechanical properties and hydrophilicity of electrospun nanofiber membranes for filtration applications by dopamine modification. J Membr Sci 460:241–249. https://doi.org/10.1016/j.memsci.2014.01.045

16. Zhao R, Li X, Sun B, et al (2017) Diethylenetriamine-assisted synthesis of amino-rich hydrothermal carbon-coated electrospun polyacrylonitrile fiber adsorbents for the removal of Cr(VI) and 2,4-dichlorophenoxyacetic acid. J Colloid Interface Sci 487:297–309. https://doi.org/10.1016/j.jcis.2016.10.057

17. Na H, Li Q, Sun H, et al (2009) Anisotropic mechanical properties of hot-pressed PVDF membranes with higher fiber alignments via electrospinning. Polym Eng Sci 49:1291–1298. https://doi.org/10.1002/pen.21368

18. Chen Y, Wang N, Jensen M, Li X (2022) Low-temperature welded PAN/TPU composite nanofiber membranes for water filtration. J Water Process Eng 47:102806. https://doi.org/10.1016/j.jwpe.2022.102806

19. Xin R, Ma H, Venkateswaran S, Hsiao BS (2021) Electrospun Nanofibrous Adsorption Membranes for Wastewater Treatment: Mechanical Strength Enhancement. Chem Res Chin Univ 37:355–365. https://doi.org/10.1007/s40242-021-1095-5

20. Woo YC, Tijing LD, Shim W-G, et al (2016) Water desalination using graphene-enhanced electrospun nanofiber membrane via air gap membrane distillation. J Membr Sci 520:99–110. https://doi.org/10.1016/j.memsci.2016.07.049

21. Augustine R, Malik HN, Singhal DK, et al (2014) Electrospun polycaprolactone/ZnO nanocomposite membranes as biomaterials with antibacterial and cell adhesion properties. J Polym Res 21:347. https://doi.org/10.1007/s10965-013-0347-6

22. Pascariu Dorneanu P, Cojocaru C, Samoila P, et al (2018) Novel fibrous composites based on electrospun PSF and PVDF ultrathin fibers reinforced with inorganic nanoparticles: Evaluation as oil spill sorbents. Polym Adv Technol 29:1435–1446. https://doi.org/10.1002/pat.4255

23. Januariyasa IK, Ana ID, Yusuf Y (2020) Nanofibrous poly(vinyl alcohol)/chitosan contained carbonated hydroxyapatite nanoparticles scaffold for bone tissue engineering. Mater Sci Eng C 107:110347. https://doi.org/10.1016/j.msec.2019.110347

24. He B, Tian L, Li J, Pan Z (2013) Effect of hot-stretching on morphology and mechanical properties of electrospun PMIA nanofibers. Fibers Polym 14:405–408. https://doi.org/10.1007/s12221-013-0405-z

25. Hou X, Yang X, Zhang L, et al (2010) Stretching-induced crystallinity and orientation to improve the mechanical properties of electrospun PAN nanocomposites. Mater Des 31:1726–1730. https://doi.org/10.1016/j.matdes.2009.01.051

26. Ji J, Sui G, Yu Y, et al (2009) Significant Improvement of Mechanical Properties Observed in Highly Aligned Carbon-Nanotube-Reinforced Nanofibers. J Phys Chem C 113:4779–4785. https://doi.org/10.1021/jp8077198

27. Yoon K, Hsiao BS, Chu B (2009) Formation of functional polyethersulfone electrospun membrane for water purification by mixed solvent and oxidation processes. Polymer 50:2893–2899. https://doi.org/10.1016/j.polymer.2009.04.047

28. Liu X, Ma H, Hsiao BS (2019) Interpenetrating Nanofibrous Composite Membranes for Water Purification. ACS Appl Nano Mater 2:3606–3614. https://doi.org/10.1021/acsanm.9b00565

29. Sun M, Li X, Ding B, et al (2010) Mechanical and wettable behavior of polyacrylonitrile reinforced fibrous polystyrene mats. J Colloid Interface Sci 347:147–152. https://doi.org/10.1016/j.jcis.2010.03.026

30. Li H, Zhu C, Xue J, et al (2017) Enhancing the Mechanical Properties of Electrospun Nanofiber Mats through Controllable Welding at the Cross Points. Macromol Rapid Commun 38:1600723. https://doi.org/10.1002/marc.201600723

31. Bae J, Baek I, Choi H (2016) Mechanically enhanced PES electrospun nanofiber membranes (ENMs) for microfiltration: The effects of ENM properties on membrane performance. Water Res 105:406–412. https://doi.org/10.1016/j.watres.2016.09.020

32. Huang L, Manickam SS, McCutcheon JR (2013) Increasing strength of electrospun nanofiber membranes for water filtration using solvent vapor. J Membr Sci 436:213–220. https://doi.org/10.1016/j.memsci.2012.12.037

33. Wu S-H, Qin X-H (2013) Uniaxially aligned polyacrylonitrile nanofiber yarns prepared by a novel modified electrospinning method. Mater Lett 106:204–207. https://doi.org/10.1016/j.matlet.2013.05.010

34. Yu L, Shao Z, Xu L, Wang M (2017) High Throughput Preparation of Aligned Nanofibers Using an Improved Bubble-Electrospinning. Polymers 9:658. https://doi.org/10.3390/polym9120658

35. Han X, Huang Z, He C, et al (2008) Coaxial electrospinning of PC(shell)/PU(core) composite nanofibers for textile application. Polym Compos 29:579–584. https://doi.org/10.1002/pc.20180

36. Cai R, Zhou Y, Hu J, et al (2022) A novel sodium alginate/cellulose nanofiber self-supported hydrogel membrane and its filtration performance. J Water Process Eng 50:103303. https://doi.org/10.1016/j.jwpe.2022.103303

37. Homaeigohar SSh, Buhr K, Ebert K (2010) Polyethersulfone electrospun nanofibrous composite membrane for liquid filtration. J Membr Sci 365:68–77. https://doi.org/10.1016/j.memsci.2010.08.041

38. Barani M, Riahi CH, Heidari V, Bazgir S (2022) Pilot-scale continuous bacterial filtration using nanofibrous filters. J Water Process Eng 48:102925. https://doi.org/10.1016/j.jwpe.2022.102925

39. Lev J, Holba M, Kalhotka L, et al (2012) Improvements in the Structure of Electrospun Polyurethane Nanofibrous Materials Used for Bacterial Removal from Wastewater. Int J Theor Appl Nanotechnol. https://doi.org/10.11159/ijtan.2012.003

40. Sumin L, Kimura D, Yokoyama A, et al (2009) The Effects of Laundering on the Mechanical Properties of Mass-produced Nanofiber Web for Use in Wear. Text Res J 79:1085–1090. https://doi.org/10.1177/0040517508101622

41. Sumin L, Kimura D, Keun Hyung Lee, et al (2010) The Effect of Laundering on the Thermal and Water Transfer Properties of Mass-produced Laminated Nanofiber Web for Use in Wear. Text Res J 80:99–105. https://doi.org/10.1177/0040517508102308

42. Pervez MN, Talukder ME, Mishu MR, et al (2022) Fabrication of polyethersulfone/polyacrylonitrile electrospun nanofiber membrane for food industry wastewater treatment. J Water Process Eng 47:102838. https://doi.org/10.1016/j.jwpe.2022.102838

43. Ke X, Ribbens S, Fan Y, et al (2011) Integrating efficient filtration and visible-light photocatalysis by loading Ag-doped zeolite Y particles on filtration membrane of alumina nanofibers. J Membr Sci 375:69–74. https://doi.org/10.1016/j.memsci.2011.02.024

44. Ma H, Yoon K, Rong L, et al (2010) High-flux thin-film nanofibrous composite ultrafiltration membranes containing cellulose barrier layer. J Mater Chem 20:4692. https://doi.org/10.1039/b922536f

45. Ma H, Yoon K, Rong L, et al (2010) Thin-Film Nanofibrous Composite Ultrafiltration Membranes Based on Polyvinyl Alcohol Barrier Layer Containing Directional Water Channels. Ind Eng Chem Res 49:11978–11984. https://doi.org/10.1021/ie100545k

46. Yu J, Kim Y-G, Kim DY, et al (2015) Super high flux microfiltration based on electrospun nanofibrous m-aramid membranes for water treatment. Macromol Res 23:601–606. https://doi.org/10.1007/s13233-015-3086-1

47. Haider S, Park S-Y (2009) Preparation of the electrospun chitosan nanofibers and their applications to the adsorption of Cu(II) and Pb(II) ions from an aqueous solution. J Membr Sci 328:90–96. https://doi.org/10.1016/j.memsci.2008.11.046

48. Ahsani M, Oghyanous FA, Meyer J, et al (2022) PVDF membranes modified with diblock copolymer PEO-b-PMMA as additive: Effects of copolymer and barrier pore size on filtration performance and fouling in a membrane bioreactor. Chem Eng Res Des 184:678–691. https://doi.org/10.1016/j.cherd.2022.05.051

49. Yuan X-T, Wu L, Geng H-Z, et al (2021) Polyaniline/polysulfone ultrafiltration membranes with improved permeability and anti-fouling behavior. J Water Process Eng 40:101903. https://doi.org/10.1016/j.jwpe.2020.101903

50. Nasir AM, Awang N, Jaafar J, et al (2021) Recent progress on fabrication and application of electrospun nanofibrous photocatalytic membranes for wastewater treatment: A review. J Water Process Eng 40:101878. https://doi.org/10.1016/j.jwpe.2020.101878

51. Serra T, Barcelona A, Pous N, et al (2022) Disinfection and particle removal by a nature-based Daphnia filtration system for wastewater treatment. J Water Process Eng 50:103238. https://doi.org/10.1016/j.jwpe.2022.103238

52. Kimmer D, Vincent I, Lev J, et al (2013) Nanofiber structures in bacteria deactivation and removal from wastewater and polluted air. In: Conference proceedings FILTECH 2013. Filtech Exhibitions Germany GmbH & Co KG, Meerbusch, Germany, Wiesbaden, Germany, p 12

53. Barhate R, Ramakrishna S (2007) Nanofibrous filtering media: Filtration problems and solutions from tiny materials. J Membr Sci 296:1–8. https://doi.org/10.1016/j.memsci.2007.03.038

54. Ma H, Burger C, Hsiao BS, Chu B (2011) Ultra-fine cellulose nanofibers: new nano-scale materials for water purification. J Mater Chem 21:7507. https://doi.org/10.1039/c0jm04308g

55. Kimmer D, Vincent I, Lovecká L, et al CZ Patent No.308593 Method of manufacturing a filter membrane